scientific reports

Check for updates

OPEN

Profiling of metabolic dysregulation in ovarian cancer tissues and biofluids

Tsuyoshi Ohta[1]✉, Masahiro Sugimoto[2], Yasufumi Ito[1], Shota Horikawa[1], Yosuke Okui[1], Hirotsugu Sakaki[1], Manabu Seino[1], Makoto Sunamura[3] & Satoru Nagase[1]

Ovarian cancer (OC) is the most lethal gynecologic cancer, mainly due to late diagnosis with widespread peritoneal spread at first presentation. We performed metabolomic analyses of ovarian and paired control tissues using capillary electrophoresis-mass spectrometry and liquid chromatography-mass spectrometry to understand its metabolomic dysregulation. Of the 130 quantified metabolites, 96 metabolites of glycometabolism, including glycolysis, tricarboxylic acid cycles, urea cycles, and one-carbon metabolites, showed significant differences between the samples. To evaluate the local and systemic metabolomic differences in OC, we also analyzed low or non-invasively available biofluids, including plasma, urine, and saliva collected from patients with OC and benign gynecological diseases. All biofluids and tissue samples showed consistently elevated concentrations of N^1,N^{12}-diacetylspermine compared to controls. Four metabolites, polyamines, and betaine, were significantly and consistently elevated in both plasma and tissue samples. These data indicate that plasma metabolic dysregulation, which the most reflected by those of OC tissues. Our metabolomic profiles contribute to our understanding of metabolomic abnormalities in OC and their effects on biofluids.

Keywords Ovarian cancer, Metabolomic dysfunction, Cancer tissues, Normal tissue, Biofluids

Metabolomic reprogramming of cancer cells is cancer hallmarks and is acquired during its multistep development[1]. Metabolomic alterations such as increased rates of glycolysis, glutaminolysis and lipid synthesis in cancer provide a foundation for sustained tumor growth[2]. Metabolites are the end products of the complex effects of the actions of genes, proteins, and enzymes, as well as environmental exposure, and they reflect the disease phenotype[3,4]. Metabolomics can provide measurements of large numbers of metabolites in cells, tissues or biological fluids, and is used in studies including targeted analysis, metabolomic profiling, and fingerprinting[5,6].

Ovarian cancer (OC) is the most lethal gynecological cancer, mainly due to late diagnosis accompanied by widespread peritoneal dissemination at first presentation. The 5-year survival rate of patients with distant metastases and disease localized to the ovary is 31.5% and 92.4%, respectively[7]; therefore, early diagnosis is crucial to improve patient prognosis. CA-125 and transvaginal sonography (TVS) are commonly used for OC screening. However, a meta-analysis of clinical trials showed that screening for CA-125 and/or TVS did not decrease OC mortality[8]. Recently, metabolomics has been used to identify new biomarkers and investigate the pathogenesis of OC. Mass spectrometric metabolomic profiling of plasma in combination with CA-125 allows early detection of OC with high sensitivity[9]. Metabolomic profiling of 448 plasma samples related to OC identified piperine, 3-indolepropionic acid, 5-hydroxyindoleacetaldehyde, and hydroxyphenyllactate as OC metabolic biomarkers[10]. These metabolites could distinguish OC from benign ovarian tumors and uterine fibroids, and early-stage disease from late-stage disease. Another study using metabolomics of plasma, ascites and tumor tissues showed that low serum phospholipids and essential amino acids were predictors of worse survival in OC[11]. These findings suggest that exploring the metabolic characteristics of biological samples could facilitate early diagnosis and aid in understanding the underlying biological mechanisms of OC. Several previous studies focusing on metabolomic profiling for OC have evaluated blood[9,10,12], urine[13,14], and tissue[15–17] separately as biological samples. Currently, salivary metabolomics is a well-established, novel, and non-invasive biological sampling technique. It has been used to distinguish patients with breast, pancreatic, and oral cancer[18–20]. However, whether metabolomic changes in tumors correlate with measurable changes in metabolites in the blood, urine, and saliva remains unknown.

[1]Department of Obstetrics and Gynecology, Faculty of Medicine, Yamagata University, Yamagata 990-9585, Japan. [2]Institute for Advanced Biosciences, Keio University, Tsuruoka, Yamagata 997-0052, Japan. [3]Department of Intestinal Surgery Medical Center, Tokyo Medical University, Hachioji, Tokyo 193-0998, Japan. ✉email: oota-t@med.id.yamagata-u.ac.jp

This study aimed to evaluate the local and systemic metabolomic differences in OC using targeted metabolomics of tumor tissues, preoperative plasma, urine, and saliva, and to identify the best biofluid associated with metabolic changes in tumors.

Results

Patient characteristics

Table 1 presents the participant characteristics, including 37 patients with ovarian cancer (OC) and 30 patients with benign gynecological diseases, defined as controls (C). The median ages of the OC and C groups were 52 (33–86) and 43 (25–71), respectively. The two groups had no significant difference in median body mass index (BMI). No significant difference was observed in the proportion of diabetes, hyperlipidemia, and smokers between the two groups. The sample numbers of International Federation of Gynecology and Obstetrics (FIGO) I, II, III, and IV were 20, seven, nine and one, respectively. The histological types of OC included nine high-grade serous carcinomas, 10 endometrioid carcinomas, 14 clear cell carcinomas, two mucinous carcinomas, one carcinosarcoma, and one small cell carcinoma. The C group consisted of eight benign ovarian tumors, 19 uterine myomas, one adenomyosis, one poly cystic ovary syndrome (PCOS), and one sterility.

Metabolic profile of ovarian cancer and normal tissues

Of the OC samples ($n=37$), 24 paired ovarian tumor (OT) and normal tissues (NT) were used for subsequent analyses. Metabolomic analyses quantified 130 metabolites in the tissue samples. In totally, 96 metabolites significantly different between the OT and NT groups (Fig. 1A). Most of the metabolites showed higher concentrations in the OT group, including N^1,N^{12}-diacetylspermine, UDP-*N*-acetylglucosamine, and adenosine monophosphate (AMP), whearas only nine metabolites showed lower concentrations, such as phosphoenolpyruvate (PEP). The heat map shows the metabolomic profiles of the individual samples (Fig. 1B).

Multivariate analyses also revealed apparent profile-level differences between the OT and NT groups. The score and loading plots of the PCA are illustrated in Figure S1A and S1B, respectively. Score plots of PLS-DA and variable importance of prediction (VIP) scores are also shown in Figure S1C and S1D, respectively. For example, guanosine monophosphate (GMP) contributed the most to the separation according to the VIP score. The histological subtype and clinical stage had no apparent profile-level difference (Figures S2).

The pathway analysis revealed pathway-level differences between the two groups (Fig. 1C). The significantly different pathways included glucose and amino acids metabolism, such as (1) pyruvate metabolism, (2) glycolysis/gluconeogenesis, (3) propanoate metabolism, (4) amino sugar and nucleotide sugar metabolism, (5) citrate cycle (TCA cycle), and (6) glycine, serine and threonine metabolism (Table 2). Individual data, including glucose metabolism and related pathways, were visualized in a pathway form (Fig. 2). Except for the two intermediate metabolites in glycolysis, most metabolites showed higher concentrations in the OT group.

	Ovarian cancer	Control	*p*-value
Number of patients	37	30	
Age (median, range)	52 (33–86)	43 (25–71)	< 0.0001
BMI (median, range)	22.2 (18.5–34.1)	22.15 (19.4–35)	0.421
Diabetes	1 (2.7%)	1 (3.3%)	1
Hyperlipidemia	6 (16.2%)	2 (6.6%)	0.281
Smoking habit	4 (10.8%)	7 (23.3%)	0.199
Stage			
I	20 (54.0%)		
II	7 (18.9%)		
III	9 (24.3%)		
IV	1 (2.7%)		
Histological type			
High grade serous carcinoma	9 (24.3%)		
Endometrioid carcinoma	10 (27.0%)		
Clear cell carcinoma	14 (37.8%)		
Mucinous carcinoma	2 (5.4%)		
Carcinosarcoma	1 (2.7%)		
Small cell carcinoma	1 (2.7%)		
Disease			
Ovarian tumor (benign)		8 (26.6%)	
Uterine myoma		19 (63.3%)	
Adenomyosis		1 (3.3%)	
PCOS		1 (3.3%)	
Sterility		1 (3.3%)	

Table 1. Characteristics of subjects.

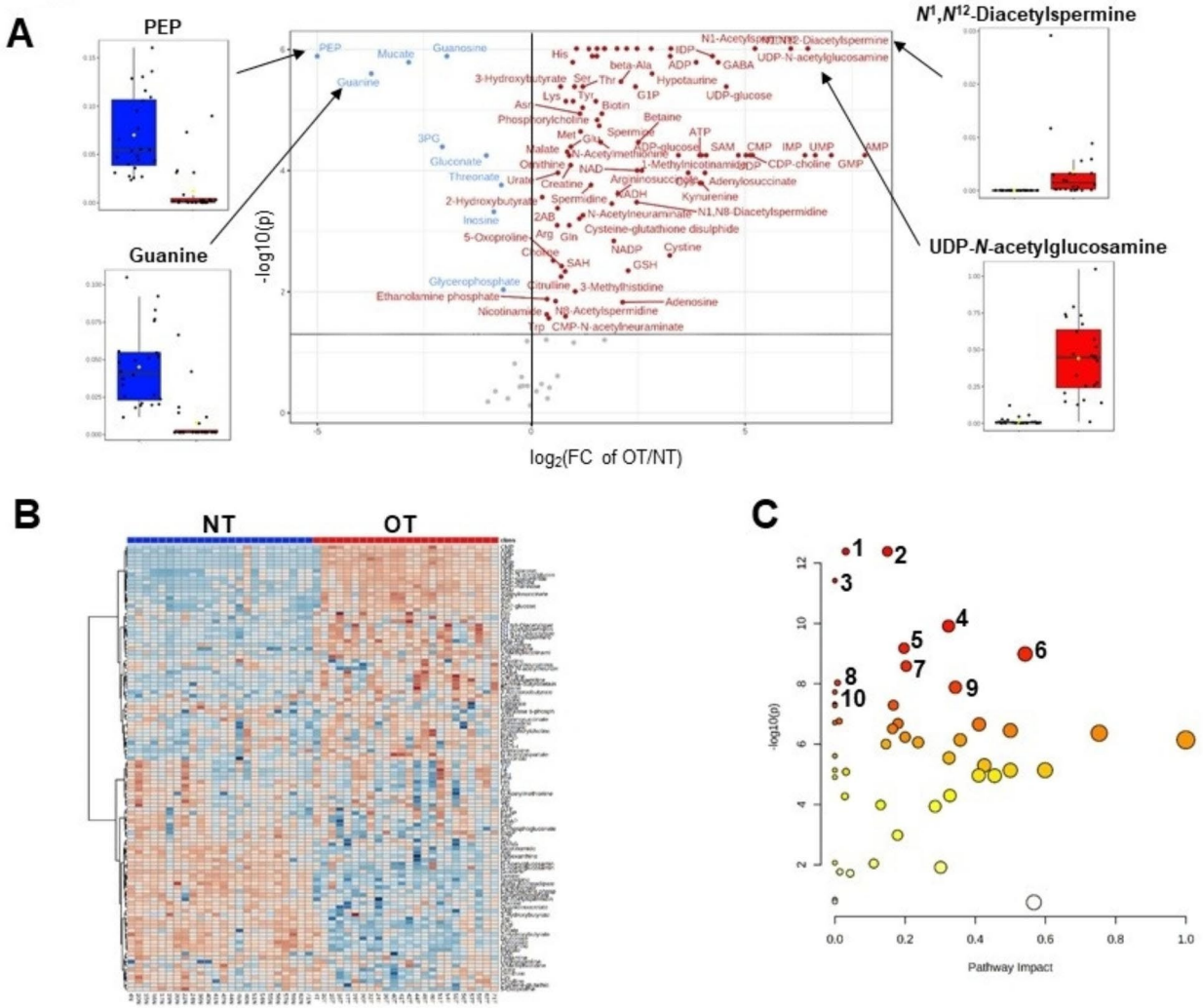

Fig. 1. Metabolomic profile of paired tumor (T) and normal (N) tissues. (**A**) Volcano plot of metabolite concentrations (μmol/g). X-axis indicates the $\log_2$-fold change (FC) of the averaged values of (T/N). Y-axis indicates the $-\log_{10}$(P-value) (Wilcoxon test corrected by FDR). Metabolites showing $Y > 1.3$, i.e., $P < 0.05$, were colored red or blue. Resentative metabolites were shown in box plots. (**B**) Heatmap of each metabolite's higher (red) and lower (blue) concentration. Normalization by the sum, log transformation, and auto-scaling were used as options for data processing. Elucidation distance was used for clustering. (**C**) Pathway analysis. No normalization was used for data processing. X and Y-axes indicate the pathway impact and $-\log_{10}$(P-value). Ten representative pathways were labeled. (1) Pyruvate metabolism. (2) Glycolysis / Gluconeogenesis. (3) Propanoate metabolism. (4) Amino sugar and nucleotide sugar metabolism. (5) Citrate cycle (TCA cycle). (6) Glycine, serine and threonine metabolism. (7) Pentose and glucuronate interconversions. (8) Primary bile acid biosynthesis. (9) Cysteine and methionine metabolism. (10) Selenocompound metabolism.

Metabolic profile of biofluid samples

Plasma sample analyses quantified 84 metabolites and revealed that seven metabolites differed significantly between OC and C groups (Fig. 3A). For example, betaine and N^1,N^{12}-diacetylspermine had higher concentrations in the OC, whereas 4-methyl-2-oxopentanoate and histidine (His) had lower concentrations. A heat map of plasma metabolic profiles is shown in Fig. 3B.

Urine sample analyses quantified 140 metabolites, of which 10 metabolites showed significant differences between the two groups (Fig. 4A and B). Salivary sample analyses quantified 82 metabolites and revealed that 50 metabolites differed significantly between the two groups (Fig. 5A and B). In these samples, all significantly different metabolites showed high OC concentrations.

Metabolites consistently different among three biofluids and tissue samples

The number of metabolites showing significantly different concentrations between OT and NT samples and between OC and C plasma samples is shown in Fig. 6A. In totally, 12 metabolites were significantly different ($P < 0.05$) in both samples, and five metabolites were significantly different using an FDR-corrected $P < 0.05$.

Rank	Pathway	Number of total compounds	Hits	Raw *p*-value	-LOG10 *p*-value	Holm adjust	FDR	Impact
1	Pyruvate metabolism	22	4	4.13E-13	12.384	2.02E-11	1.01E-11	0.0311
2	Glycolysis / Gluconeogenesis	26	5	4.13E-13	12.384	2.02E-11	1.01E-11	0.14972
3	Propanoate metabolism	23	3	3.81E-12	11.419	1.79E-10	6.22E-11	0
4	Amino sugar and nucleotide sugar metabolism	37	10	1.23E-10	9.9118	5.64E-09	1.50E-09	0.32396
5	Citrate cycle (TCA cycle)	20	5	6.63E-10	9.1787	2.98E-08	6.49E-09	0.19704
6	Glycine, serine and threonine metabolism	33	9	1.03E-09	8.9874	4.53E-08	8.41E-09	0.54222
7	Pentose and glucuronate interconversions	18	4	2.60E-09	8.585	1.12E-07	1.82E-08	0.20312
8	Primary bile acid biosynthesis	46	1	9.29E-09	8.0319	3.90E-07	5.69E-08	0.00758
9	Cysteine and methionine metabolism	33	8	1.31E-08	7.8821	5.38E-07	7.14E-08	0.34331
10	Selenocompound metabolism	20	1	1.88E-08	7.7252	7.53E-07	9.23E-08	0

Table 2. Pathway ranking for tissue. FDR, false discovery rate.

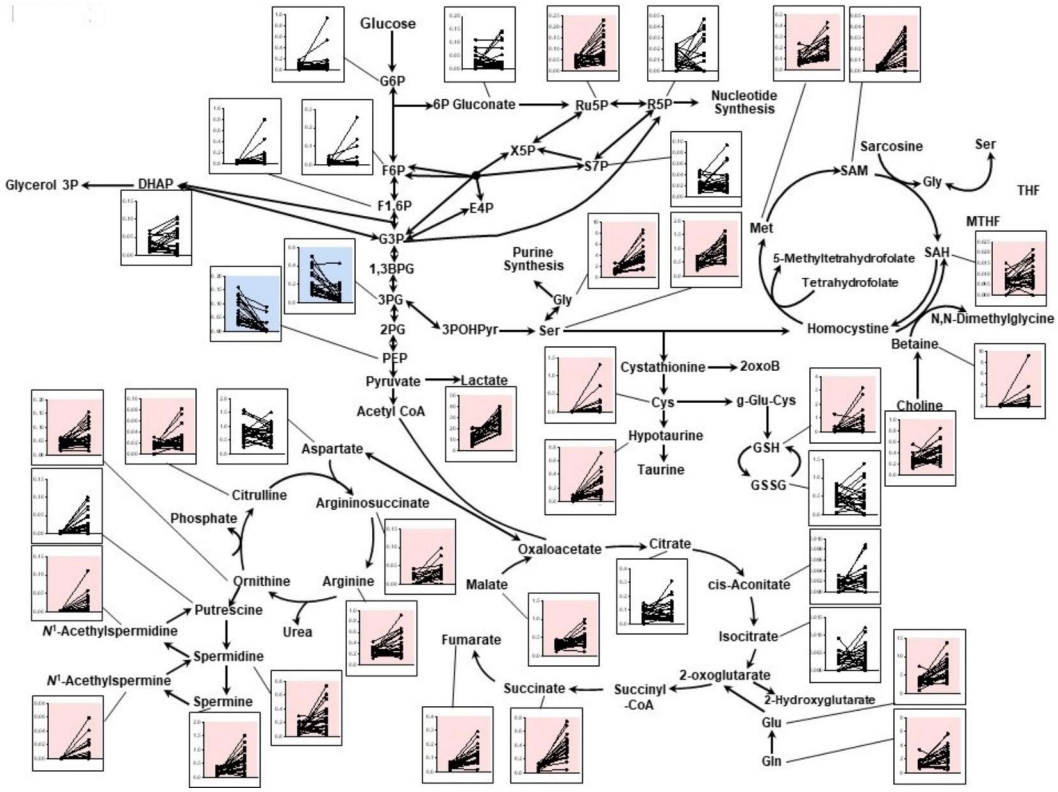

Fig. 2. Pathway visualization of metabolomic concentrations in paired ovarian tumor (OT) and normal tissues (NT). Individual data were visualized in dot plots. The left and right plots are the data of NT and OT. The metabolites showing $P < 0.05$ (Wilcoxon test corrected by FDR) were colored pink (higher in OT) and light blue (lower in OT). The Y-axis indicates the metabolite concentration (μmol/g).

(Table S1). Two acetylated polyamines, –*N*-acetylasparate, betaine and His–were also included. Four of these metabolites were consistently elevated in the OT and OC groups (Figure S3).

The number of metabolites showing significantly different concentrations between OC and C in the three types of biofluids is shown in Fig. 6B. N^1,N^{12}-diacetylspermine levels were consistently elevated in the biofluids. The discriminatory abilities of this metabolite for tissues (OT vs. NT) and biofluids (OC vs. C) is shown in Fig. 6C. The AUC value for the tissue sample was the highest at 0.950 (95% confidence interval [CI]: 0.889−1.000). The AUCs for plasma and urine were similar: 0.734 (95% CI: 0.612−0.857) for plasma and 0.755 (95% CI: 0.633−0.876) for urine. The saliva showed the lowest value; 0.681 (95% CI: 0.547−0.815).

Discussion

This study is the first study to systematically investigate metabolic changes between OT and NT in tissue samples, and OC and C in plasma, urine, and saliva samples. Most previous studies have used one or two biological

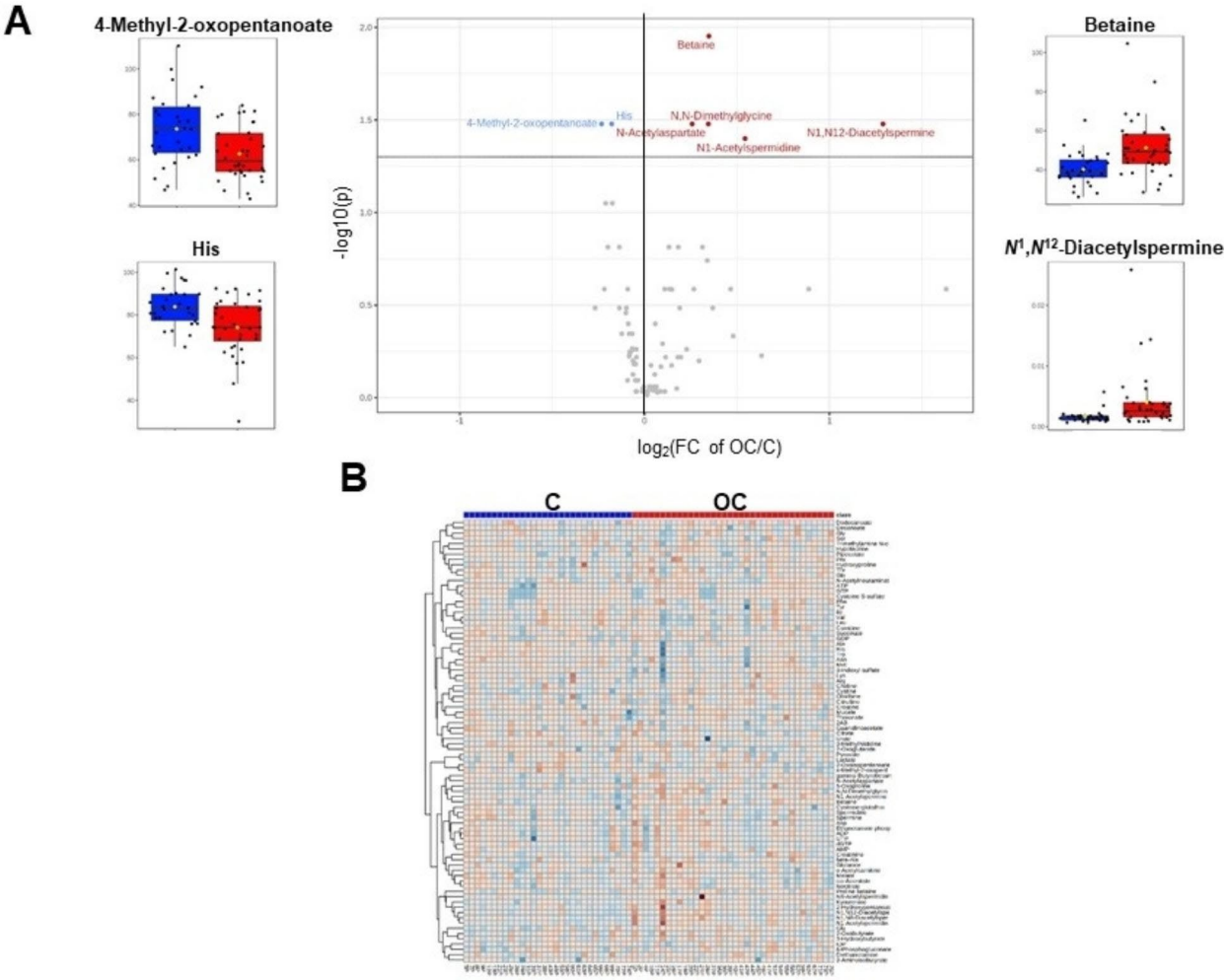

Fig. 3. Metabolomic profiles in plasma collected from the patients with ovarian cancer (OC) and controls (C). (**A**) Volcano plot of metabolite concentrations (μmol/g). X-axis indicates the $\log_2$-fold change (FC) of the averaged values of (OC/C). Y-axis indicates the $-\log_{10}$(P-value) (Wilcoxon test corrected by FDR). Representative metabolites were shown in box plots. (**B**) Heatmap visualization.

samples for metabolic analysis to achieve early diagnosis and understand the underlying biological mechanisms of ovarian cancer.

Our metabolomic profiling of 24 paired OT and NT samples showed that the accumulation of lactate, an end product of glycolysis, and the reduction of intermediate metabolites in glycolysis, such as PEP and glycerate 3-phosphate (3PG) in OT (Figs. 1A and 2), indicating that the Warburg effect, a well-known characteristic of cancer cell energy metabolism, was observed in OC tissues. The glutamine and glutamic acid levels were significantly higher in the OT group than the NT group. Levels of metabolites in the latter half of the TCA cycle, such as succinate, fumarate, and malate, were significantly elevated in the OT group (Figs. 1A and 2). The activation of glycolysis and glutaminolysis in OC tissues is consistent with previous studies that performed metabolic analyses using various cancer tissues[20–22]. One-carbon metabolism, including that of choline, betaine, methionine, S-adenosylmethionine (SAM), and S-adenosylhomocysteine (SAH) was higher in the OT group (Figs. 1A and 2). The metabolites produced are made available for nucleotide biosynthesis, methylation, regulation of redox status, which contribute to cell proliferation, chemoresistance, and survival in OC[23]. In our paired tissue samples, metabolites associated with the urea cycle and polyamine pathway were elevated in the OT group compared to those in the NT group (Figs. 1A and 2). These results are consistent with that of a previous study which investigated metabolic alterations in unpaired normal ovarian and primary OC tissues[22]. The alterations in the urea cycle are also associated with cancer progression[24]. Notably, polyamines have been reported to be more abundant in high-grade serous carcinomas (HGSC) than in non-HGCS[17], implying that the polyamine pathway may be involved in the aggressive phenotype of OC.

To identify the best biofluid reflecting metabolic dysregulation in OC tissues, we compared the metabolomic profiles of plasma, urine, and saliva between OC and C groups. The number of metabolites showing significantly

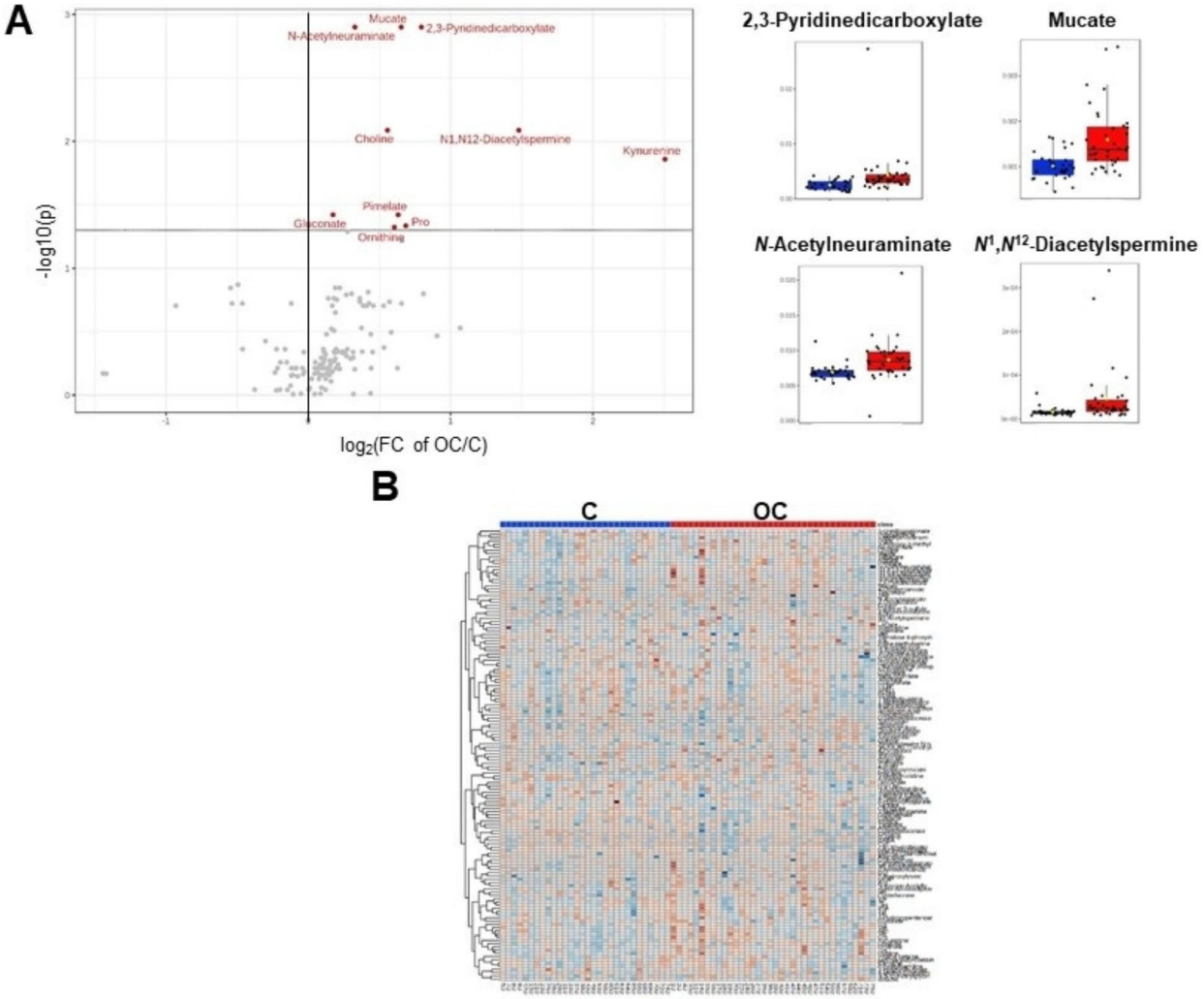

Fig. 4. Metabolic profiles in urine. (**A**) Volcano plot of metabolite concentrations (no unit). X-axis indicates the $\log_2$-fold change (FC) of the averaged values of (OC/C). Y-axis indicates the $-\log_{10}$(P-value) (Wilcoxon test corrected by FDR). Representative metabolites were shown in box plots. (**B**) Heatmap visualization. Urinary metabolite concentration was calculated by dividing the creatinine concentration of each sample.

different concentrations in three types of biofluids between the two groups was less than that between the OT and NT groups in the tissue samples (Figs. 3A and 4A, and 5). Our metabolic profiling demonstrated that plasma could be the best biofluid to reflect metabolic dysregulation in OC tissues. In totally, 12 metabolites showed consistently significant differences in both the plasma and tissue samples (Supplementary Table S1). Four metabolites, His, Leu, Met, and Trp, showed higher concentrations in OT but not in plasma samples, indicating that these metabolites might be actively taken up from the plasma into the tissues. N^1,N^{12}-diacetylspermine was consistently elevated in cancer tissues and the three types of biofluids (Figs. 1A and 6B). The discriminant abilities of this metabolite for tissues (OT from NT) and the biofluids (OC from C) were significant (Fig. 6C). Elevation of N^1,N^{12}-diacetylspermine, a polyamine metabolite, indicates that the polyamine pathway may play an essential role in OC metabolism. Elevated polyamine levels are involved in the initial stage of neoplastic transformation and tumor progression[25,26]. Previous studies have reported that plasma polyamines are useful for detecting early-stage OC[9], and urinary polyamines can distinguish between benign and malignant ovarian tumors in both early and advanced stage[13]. Ornithine decarboxylase (ODC) is the first enzyme in the polyamine synthesis pathway in mammals and is transcriptionally regulated by MYC[27,28]. Integrated genome analysis has demonstrated that MYC is amplified in 30–40% of human ovarian tumors[29], thereby linking the polyamine pathway and OC carcinogenesis via MYC. Moreover, the interaction between polyamine metabolism and other cancer-driving pathways, including the PTEN-PI3K-mTOR, WNT signaling and RAS pathways, suggests that the polyamine pathway is a potential therapeutic target[30]. Furthermore, in malignant gliomas and colon cancers, difluoromethlyornithine (DFMO), a specific inhibitor of ODC, has progressed to clinical trials[31,32]. Similarly,

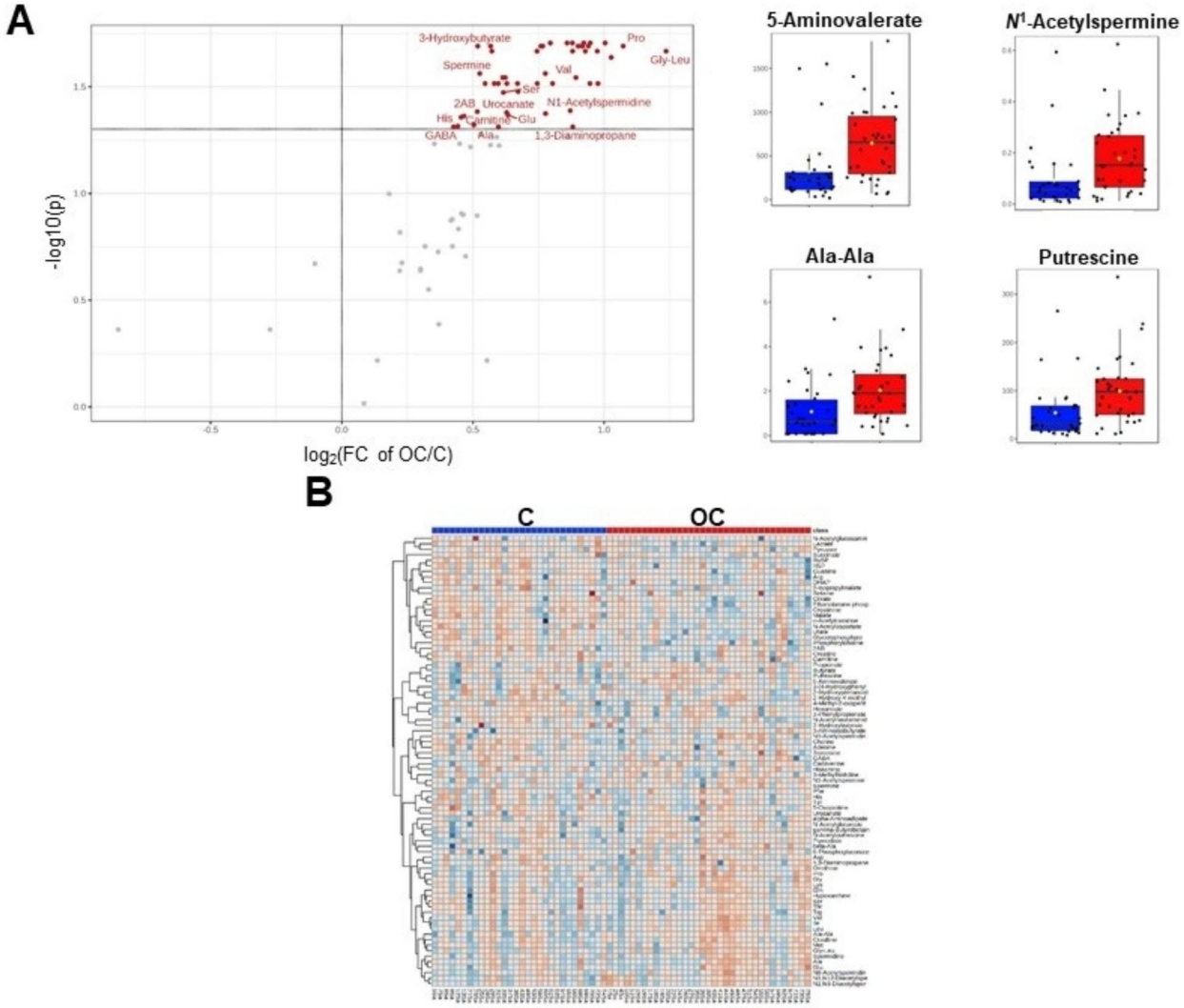

Fig. 5. Metabolic profiles in saliva. (**A**) Volcano plot of metabolite concentrations (μmol/g). X-axis indicates the $\log_2$-fold change (FC) of the averaged values of (OC/C). Y-axis indicates the $-\log_{10}$(P-value) (Wilcoxon test corrected by FDR). Resentative metabolites were shown in box plots. (**B**) Heatmap visualization.

our results showed that the polyamine pathway is activated in OC, and further study is necessary to evaluate the specificity of this activation.

Nonetheless, this study had some potential limitations. The median age in the OC group was significantly higher than that in the control group, indicating that age may be a confounding variable in our analyses. The metabolomic profiles of tissue samples were clustered to separate NT and OT rather than the age (Figure S4). The age-mapped score plots of PCA also showed no apparent age-dependent age (Figure S5). The metabolomic profiles of the plasma sample also showed no clear age-dependent cluster (Figure S6). Nevertheless, age-matched studies are preferred to avoid histological and tumor burden biases. The relationship between the metabolomic profile and prognosis was also not analyzed because of the few cases of recurrence. More extensive samples are necessary for such analyses and rigorous validations.

In summary, our metabolomic profiling of tissues, plasma, urine, and saliva demonstrated that plasma is the best biofluid for reflecting metabolic changes in OC tissues. N^1,N^{12}-diacetylspermine, a component of the polyamine metabolomic pathway, was consistently elevated in tissues and three types of biofluids, implying that polyamine pathway may play an essential role in OC metabolism.

Materials and methods

Study subjects

This study was conducted according to the study protocol and was approved by the Ethics Committee of Yamagata University School of Medicine (2019 – 385). Written informed consent was obtained from each participant prior to participation in the study. Patients with OC and benign gynecological diseases were recruited from the

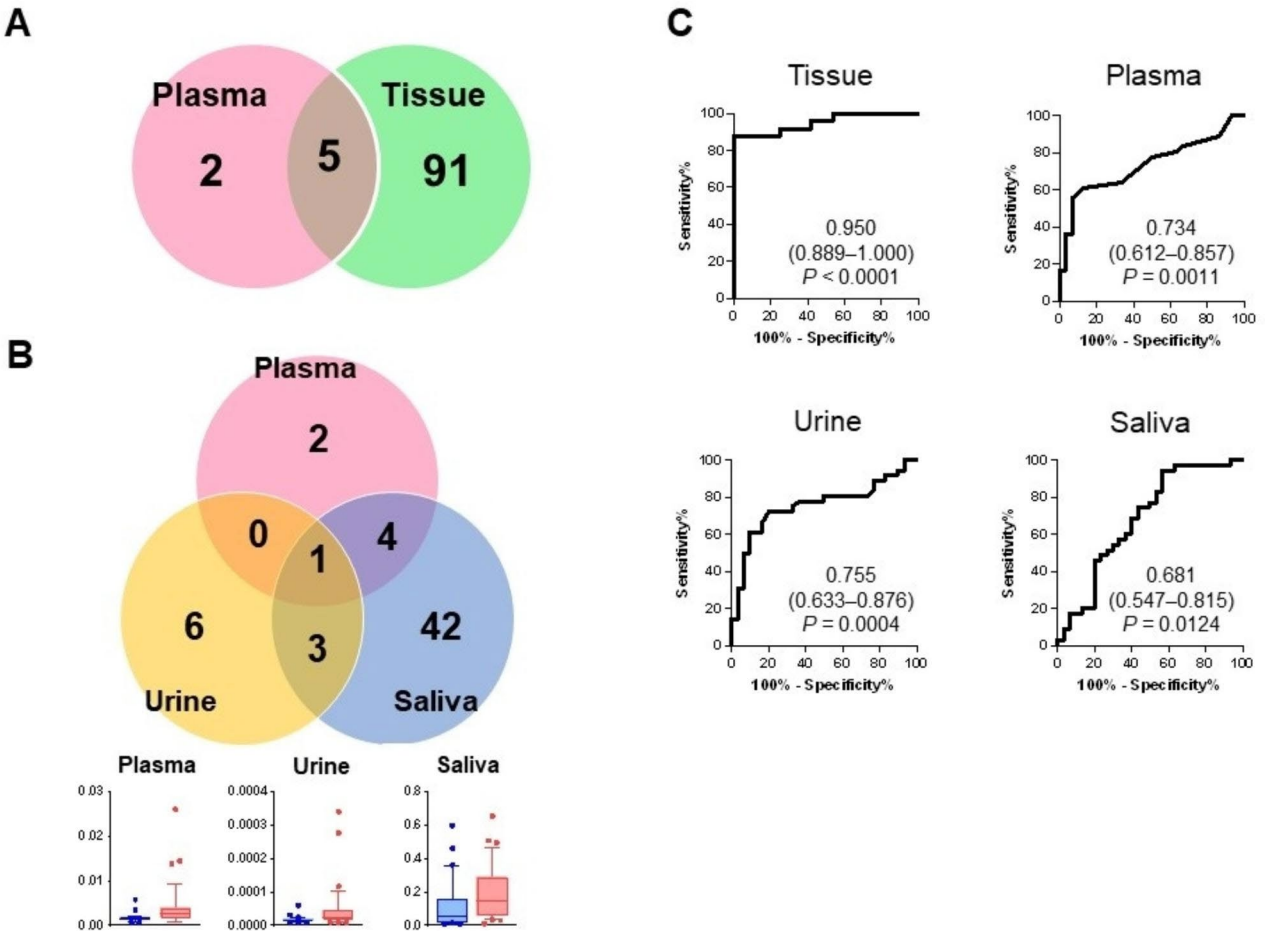

Fig. 6. Metabolites consistently elevated in tissue and multiple biofluids. (**A**) The number of significantly different metabolites between plasma and tissues (FDR-corrected P-value < 0.05). (**B**) The number of significantly different metabolites in saliva, plasma, and urine samples (FDR-corrected P-value < 0.05). (**C**) ROC curves to discriminate OT from NT (tissue) and OC from C (biofluids). AUC, 95% confidential intervals, and P-values are described.

Department of Obstetrics and Gynecology at Yamagata University Hospital between March 2020 and December 2021. None of the patients had received any prior treatment such as chemotherapy or radiotherapy. None of the patients had any history of malignancy.

Collection of tissues and biofluids

All patients with OC provided tumor and normal tissues and plasma, urine, and saliva samples. Patients with benign gynecological diseases included plasma, urine, and saliva samples. OC and normal tissues were collected during surgery. Pathologically confirmed to be cancer-free, the healthy ovary was used as normal tissues. Biofluid samples were collected from all participants between 06:00am–9:30am the day before surgery. The study participants had not eaten or drunk since the night before biofluid collection. After collection, these samples were immediately stored at − 80 °C.

Metabolomics analysis

Metabolomic analyses were conducted using capillary electrophoresis time-of-flight mass spectrometry (CE-TOFMS) and liquid chromatography triple quadrupole mass spectrometry (LC-QQQMS). CE-TOFMS was used to profile hydrophilic metabolites. LC-QQQMS was used for the highly sensitive quantification of polyamines. The parameters of analytical instruments were described for tissue samples[20] and plasma, urine, and saliva[33–35].

Sample processing for CE-TOFMS

The saliva sample (100 µl) was centrifuged through a 5-kDa-cutoff filter (Millipore, Bedford, MA, USA) at 9100 × g for at least 2.5 h at 4 °C. The filtrate (45 µl) was transferred to a 1.5-ml Eppendorf tube with 2 mM of internal standards 1 (methionine sulfone, 2-[N-morpholino]-ethanesulfonic acid [MES], D-camphol-10-sulfonic acid, sodium salt, 3-aminopyrrolidine, and trimesate), mixed by Voltex, and used for CE-TOFMS analysis.

The urine sample (20 µl) was mixed 80 µL methanol and 250 µM each of internal standards 1 and centrifuged through a 5-kDa cutoff filter (Millipore) at 9100 × g for at 30 min at 4 °C. The filtrate was used for the CE-TOFMS analysis.

Plasma sample (40 µL) was mixed with 360 µL methanol containing 20 µM each of internal standards 1. Deionized water (160 µL) and chloroform (400 µL) were added, and the solution was centrifuged at 10,000×g for 3 min at 4 °C. The upper aqueous layer was filtered through a 5-kDa cutoff filter (Millipore) at 9100×g for 180 min at 4 °C. The remaining solution was then centrifuged (960× g) for 3 h at 40 °C. Mill-Q water (40 µL) containing internal standards 2 (200 µM of 3-aminopyrrolidine and trimesate) was used for CE-TOFMS analysis.

Tissue samples (approximately 50 mg) were plunged into methanol (500 µl) containing internal standards and 20 M each of internal standard 1 and homogenized at 1500 rpm for 1 min using a Shake Master Neo (BMS, Tokyo, Japan). Chloroform (500 µl) and of Milli-Q water (200 µl) were added to of the homogenized solution (500 µl), and the mixed solution was centrifuged at 4600×g for 15 min at 4 °C. The upper aqueous layer (300 µl) was centrifugally filtered at 9100×g for 3.5 h at 4 °C through a 5-kDa cutoff filter (Millipore). The 150 µl filtrate was lyophilized and dissolved in 50 µl of Milli-Q water containing 200 µM of internal standard 2 for CE-TOFMS analysis.

Sample processing for LC-QQQMS

Either saliva (10 µl) or urine (10 µl) was mixed with methanol (90 µl) containing 149.6 mM ammonium hydroxide [1% (v/v) ammonia solution] and 0.9 µM internal standards 3 (d8-spermine, d8-spermidine, d6-N1-acetylspermidine, d3-N1-acetylspermine, d6-N1,N8-diacetylspermidine, d6-N1,N12-diacetylspermine, and 1,6-diaminohexane). After centrifugation at 15,780×g for 10 min at 4 °C, the supernatant was transferred to a fresh tube and vacuum dried. The sample was reconstituted with 90% (v/v) methanol (10 µl) and water (30 µl) and then vortexed and centrifuged at 15,780 × g for 10 min at 4 °C. The 38 10 µl of supernatant was then injected into the LC-QQQMS. The urine sample was diluted 5000 fold and processed in the manner described above for the creatinine quantification.

Plasma (30 µl) was mixed with methanol (270 µl) containing 149.6 mM ammonium hydroxide [1% (v/v) ammonia solution] and internal standard 1 (0.2 µM). After centrifugation at 15,780 × g for 10 min at 4 °C, the supernatant was transferred to a fresh tube and vacuum dried. The sample was reconstituted with 90% methanol (10 µl) and water (20 µl) and then vortexed and centrifuged at 15,780 × g for 1 min at 4 °C, and supernatant (28 µl) was then injected into the LC-QQQMS.

Tissue samples (approximately 50 mg) were plunged into methanol (500 µl) containing internal standards and 20 M each of internal standard 1 and homogenized at 1500 rpm for 1 min using a Shake Master Neo (BMS). Homogenized solution (50 µl) was mixed with methanol (100 µl) containing 149.6 mM ammonium hydroxide [1% (v/v) ammonia solution] and 0.75 µM internal standard 3, and the mixed solution was centrifuged at 4600×g for 15 min at 4 °C. The supernatant was transferred to a fresh tube and centrifuged at 9100×g for 1 h at 40 °C. The sample was reconstituted with 90% (v/v) methanol (20 µl) and water (60 µl) and then vortexed and centrifuged at 15,780 × g for 1 min at 4 °C. The sample (75 µl) was transferred to a vial for LC-QQQMS analysis.

Data processing

The raw metabolomic data were processed using MasterHands (ver. 2.19.0.1, Keio University, Yamagata, Japan) to produce a data matrix (sample × metabolite) including absolute concentrations[36]. Briefly, migration time (MT) of each metabolite peak was corrected based on internal standards. The metabolites were identified based on the corrected MT and m/z values by matching those of the standard compounds. The peak area of each metabolite was integrated and divided by that of one of the internal standards to obtain the relative area. The ratio of the relative areas of the metabolites in a sample to the standard mixture was used to calculate the absolute metabolite concentrations in the samples[37]. The absolute concentration of each metabolite for saliva and plasma was used for subsequent analyses. The concentration of each metabolite was divided by creatinine concentrations for each urine sample. The metabolite concentration was divided by each tissue sample's wet weight.

The quantitative and nominal scales of the subject characteristics were evaluated using the Mann-Whitney and Chi-square tests. Metabolite concentrations were evaluated using the Wilcoxon matched-pair test for pairs (tissue), Mann-Whitney tests, and non-paireds samples (plasma, urine, and saliva). P-values were corrected using the false discovery rate (FDR) for multiple independent tests.

The heatmap shows the relatively high (red) and low (blue) concentrations of each metabolite. Normalization by sum, log transformation, and auto-scaling (Z-score) was used for data processing. The elucidation distance was used for clustering. MetaboAnalyst (v. 5.0 and v 6.0) was used to visualize volcano plots and heatmaps and conduct principal component analysis (PCA), partial least squares-discriminant analysis (PLS-DA), and pathway analysis[38]. GraphPad Prism (v. 9.2.0, GraphPad Software, San Diego, CA, USA) and EZR (Saitama Medical Center, Jichi Medical University, Saitama, Japan) were used for all other analyses.

Data availability

The datasets generated during and/or analysed during the current study are available from the corresponding author on reasonable request.

Received: 25 January 2024; Accepted: 11 September 2024
Published online: 16 September 2024

References

1. Hanahan, D. & Weinberg, R. A. Hallmarks of cancer: The next generation. *Cell* **144**(5), 646–674. https://doi.org/10.1016/j.cell.2011.02.013 (2011).
2. Benjamin, D. I., Cravatt, B. F. & Nomura, D. K. Global profiling strategies for mapping dysregulated metabolic pathways in cancer. *Cell Metab.* **16**(5), 565–577. https://doi.org/10.1016/j.cmet.2012.09.013 (2012).
3. Azad, R. K. & Shulaev, V. Metabolomics technology and bioinformatics for precision medicine. *Brief. Bioinform.* **20**(6), 1957–1971. https://doi.org/10.1093/bib/bbx170 (2019). PMID: 29304189; PMCID: PMC6954408.
4. Jacob, M., Lopata, A. L., Dasouki, M. & Abdel Rahman, A. M. Metabolomics toward personalized medicine. *Mass Spectrom Rev.* **38**(3), 221–238. https://doi.org/10.1002/mas.21548 (2019).
5. Shulaev, V. Metabolomics technology and bioinformatics. *Brief. Bioinform.* **7**(2), 128–139. https://doi.org/10.1093/bib/bbl012 (2006).
6. Halket, J. M. et al. Chemical derivatization and mass spectral libraries in metabolic profiling by GC/MS and LC/MS/MS. *J. Exp. Bot.* **56**(410), 219–243. https://doi.org/10.1093/jxb/eri069 (2005). Epub 2004 Dec 23. PMID: 15618298.
7. The Surveillance. Epidemiology, and End Results (SEER) Program. https://seer.cancer.gov/statfacts/html/ovary.html (2023-05-29).
8. Henderson, J. T., Webber, E. M. & Sawaya, G. F. Screening for ovarian cancer: Updated evidence report and systematic review for the US preventive services task force. *JAMA.* **319**(6), 595–606. https://doi.org/10.1001/jama.2017.21421 (2018).
9. Fahrmann, J. F. et al. A MYC-Driven plasma polyamine signature for early detection of Ovarian Cancer. *Cancers (Basel).* **13**(4), 913. https://doi.org/10.3390/cancers13040913 (2021). PMID: 33671595; PMCID: PMC7927060.
10. Ke, C. et al. Large-scale profiling of metabolic dysregulation in ovarian cancer. Int J Cancer. ;136(3):516 – 26. doi: 10.1002/ijc.29010. Epub 2014 Jun 17. PMID: 24895217. (2015).
11. Bachmayr-Heyda, A. *et al.* Integrative systemic and local metabolomics with impact on survival in high-grade serous ovarian cancer. *Clin. Cancer Res.* **23**(8), 2081–2092. https://doi.org/10.1158/1078-0432.CCR-16-1647 (2017).
12. Buas, M. F. et al. Identification of novel candidate plasma metabolite biomarkers for distinguishing serous ovarian carcinoma and benign serous ovarian tumors. *Gynecol. Oncol.* **140**(1), 138–144. https://doi.org/10.1016/j.ygyno.2015.10.021 (2016). Epub 2015 Oct 30. PMID: 26521694; PMCID: PMC5310763.
13. Niemi, R. J. *et al.* Urinary polyamines as biomarkers for ovarian cancer. *Int. J. Gynecol. Cancer.* **27**(7), 1360–1366. https://doi.org/10.1097/IGC.0000000000001031 (2017).
14. Slupsky, C. M. et al. Urine metabolite analysis offers potential early diagnosis of ovarian and breast cancers. *Clin. Cancer Res.* **16**(23), 5835–5841. https://doi.org/10.1158/1078-0432.CCR-10-1434 (2010). Epub 2010 Oct 18. PMID: 20956617.
15. Denkert, C. et al. Mass spectrometry-based metabolic profiling reveals different metabolite patterns in invasive ovarian carcinomas and ovarian borderline tumors. *Cancer Res.* **66**, 10795–10804. https://doi.org/10.1158/0008-5472.CAN-06-0755 (2006).
16. Fong, M. Y., McDunn, J. & Kakar, S. S. Identification of metabolites in the normal ovary and their transformation in primary and metastatic ovarian cancer. *PLoS One.* **6**, 1–12. https://doi.org/10.1371/journal.pone.0019963 (2011).
17. Yoshida, K. et al. Metabolome analysis reveals a diversity of cancer tissues in advanced epithelial ovarian cancer. *Cancer Cell. Int.* **21**(1), 314. https://doi.org/10.1186/s12935-021-02014-7 (2021). PMID: 34134729; PMCID: PMC8207638.
18. Murata, T. et al. Salivary metabolomics with alternative decision tree-based machine learning methods for breast cancer discrimination. *Breast Cancer Res. Treat.* **177**(3), 591–601. https://doi.org/10.1007/s10549-019-05330-9 (2019). Epub 2019 Jul 8. PMID: 31286302.
19. Asai, Y. *et al.* Elevated polyamines in saliva of pancreatic cancer. *Cancers (Basel)* **10**(2), 43. https://doi.org/10.3390/cancers10020043 (2018).
20. Ishikawa, S. et al. Identification of salivary metabolomic biomarkers for oral cancer screening. *Sci. Rep.* **6**, 31520. https://doi.org/10.1038/srep31520 (2016). PMID: 27539254; PMCID: PMC4990923.
21. Satoh, K. *et al.* Global metabolic reprogramming of colorectal cancer occurs at adenoma stage and is induced by MYC. *Proc. Natl. Acad. Sci. USA* **114**(37), E7697–E7706. https://doi.org/10.1073/pnas.1710366114 (2017).
22. Fong, M. Y., McDunn, J. & Kakar, S. S. Identification of metabolites in the normal ovary and their transformation in primary and metastatic ovarian cancer. *PLoS One.* **6**(5), e19963. https://doi.org/10.1371/journal.pone.0019963 (2011). Epub 2011 May 19. PMID: 21625518; PMCID: PMC3098284.
23. Rizzo, A. *et al.* One-carbon metabolism: Biological players in epithelial ovarian cancer. *Int. J. Mol. Sci.* **19**(7), 2092. https://doi.org/10.3390/ijms19072092 (2018).
24. Keshet, R., Szlosarek, P., Carracedo, A. & Erez, A. Rewiring urea cycle metabolism in cancer to support anabolism. *Nat Rev Cancer.* **18**(10), 634–645. https://doi.org/10.1038/s41568-018-0054-z (2018).
25. Murray-Stewart, T. R., Woster, P. M. & Casero, R. A. Jr Targeting polyamine metabolism for cancer therapy and prevention. *Biochem. J.* **473**(19), 2937–2953. https://doi.org/10.1042/BCJ20160383 (2016). PMID: 27679855; PMCID: PMC5711482.
26. Gerner, E. W. & Meyskens, F. L. Jr. Polyamines and cancer: old molecules, new understanding. *Nat Rev Cancer.* **4**(10), 781–92. https://doi.org/10.1038/nrc1454 (2004).
27. Fahrmann, J. F. et al. Association between plasma diacetylspermine and tumor spermine synthase with outcome in triple negative breast cancer. *J. Natl. Cancer Inst.* **112**(6), 607–616. https://doi.org/10.1093/jnci/djz182 (2020).
28. Bachmann, A. S. & Geerts, D. Polyamine synthesis as a target of MYC oncogenes. *J. Biol. Chem.* **293**, 18757–18769 (2018).
29. Cancer Genome Atlas Research Network. Integrated genomic analyses of ovarian carcinoma. Nature. 474(7353):609 – 15. (2011). https://doi.org/10.1038/nature10166. Erratum in: Nature. 2012;490(7419):298.
30. Casero, R. A. Jr, Murray Stewart, T. & Pegg, A. E. Polyamine metabolism and cancer: treatments, challenges and opportunities. *Nat. Rev. Cancer.* **18**(11), 681–695. https://doi.org/10.1038/s41568-018-0050-3 (2018). PMID: 30181570; PMCID: PMC6487480.
31. Levin, V. A., Ictech, S. E. & Hess, K. R. Clinical importance of eflornithine (α-difluoromethylornithine) for the treatment of malignant gliomas. *CNS Oncol.* **7**(2), CNS16. https://doi.org/10.2217/cns-2017-0031 (2018).
32. Raj, K. P. et al. Role of dietary polyamines in a phase III clinical trial of difluoromethylornithine (DFMO) and sulindac for prevention of sporadic colorectal adenomas. *Br. J. Cancer.* **108**(3), 512–518. https://doi.org/10.1038/bjc.2013.15 (2013). Epub 2013 Jan 22. PMID: 23340449; PMCID: PMC3593561.
33. Iwamoto, H. et al. Metabolomic profiling of plasma, urine, and saliva of kidney transplantation recipients. *Int. J. Mol. Sci.* **23**(22), 13938. https://doi.org/10.3390/ijms232213938 (2022). PMID: 36430414; PMCID: PMC9695205.
34. Sugimoto, M. & Aizawa, Y. Metabolomics analysis of blood, urine, and saliva samples based on capillary electrophoresis-mass spectrometry. *Methods Mol Biol.* **2571**, 83–94. https://doi.org/10.1007/978-1-0716-2699-3_8 (2023).
35. Tomita, A. et al. Effect of storage conditions on salivary polyamines quantified via liquid chromatography-mass spectrometry. *Sci. Rep.* **8**(1), 12075. https://doi.org/10.1038/s41598-018-30482-x (2018). PMID: 30104641; PMCID: PMC6089938.
36. Sugimoto, M., Wong, D. T., Hirayama, A., Soga, T. & Tomita, M. Capillary electrophoresis mass spectrometry-based saliva metabolomics identified oral, breast and pancreatic cancer-specific profiles. *Metabolomics.* **6**(1), 78–95. https://doi.org/10.1007/s11306-009-0178-y (2010). Epub 2009 Sep 10. PMID: 20300169; PMCID: PMC2818837.
37. Sugimoto, M., Aizawa, Y. & Tomita, A. Data processing and analysis in liquid chromatography-mass spectrometry-based targeted metabolomics. *Methods Mol Biol.* **2571**, 241–255. https://doi.org/10.1007/978-1-0716-2699-3_21 (2023).
38. Pang, Z. *et al.* MetaboAnalyst 5.0: Narrowing the gap between raw spectra and functional insights. *Nucleic Acids Res.* **49**(W1), W388–W396. https://doi.org/10.1093/nar/gkab382 (2021).

Acknowledgements
We would like to thank Editage (www.editage.com) for English language editing.

Author contributions
T.O., M.S., M.S., and S.N. concieved this study. T.O., M.S., and S.N. initiated and managed the collaboration. T.O., Y.I., S.H., Y.O., H.S., and M.S. collected tissues and biofluid samples. T.O. and M.S. wrote the main manuscript text and prepared Table 1; Figs. 1, 2, 3, 4, 5 and 6 and Supplementary Information File. T.O. wrote the first draft of the manuscript. All authors reviewed the manuscript and agreed with the submission.

Competing interests
Masahiro Sugimoto received annual value of remuneration from Saliva Tech Co. Ldt. and Human Metabolome Technologies Inc. Masahiro Sugimoto and Makoto Sunamura received annual profit from share from Saliva Tech Co. Ldt. The other authors declare no conflict of interest.

Ethical approval
The study protocol was approved by the Ethics Committee of Yamagata University School of Medicine (2019 – 385). All informed consent was obtained from each participant prior to participation in the study.

Additional information
Supplementary Information The online version contains supplementary material available at https://doi.org/10.1038/s41598-024-72938-3.

Correspondence and requests for materials should be addressed to T.O.

Reprints and permissions information is available at www.nature.com/reprints.

Publisher's note Springer Nature remains neutral with regard to jurisdictional claims in published maps and institutional affiliations.